

Natural Forest Biomass Estimation Based on Plantation Information Using PALSAR Data

Ram Avtar^{1,2,3*}, Rikie Suzuki², Haruo Sawada¹

1 Institute of Industrial Science, The University of Tokyo, Tokyo, Japan, **2** Research Institute for Global Change, Japan Agency for Marine-Earth Science and Technology, Yokohama, Japan, **3** United Nations University Institute for Sustainability and Peace, Tokyo, Japan

Abstract

Forests play a vital role in terrestrial carbon cycling; therefore, monitoring forest biomass at local to global scales has become a challenging issue in the context of climate change. In this study, we investigated the backscattering properties of Advanced Land Observing Satellite (ALOS) Phased Array L-band Synthetic Aperture Radar (PALSAR) data in cashew and rubber plantation areas of Cambodia. The PALSAR backscattering coefficient (σ^0) had different responses in the two plantation types because of differences in biophysical parameters. The PALSAR σ^0 showed a higher correlation with field-based measurements and lower saturation in cashew plants compared with rubber plants. Multiple linear regression (MLR) models based on field-based biomass of cashew (C-MLR) and rubber (R-MLR) plants with PALSAR σ^0 were created. These MLR models were used to estimate natural forest biomass in Cambodia. The cashew plant-based MLR model (C-MLR) produced better results than the rubber plant-based MLR model (R-MLR). The C-MLR-estimated natural forest biomass was validated using forest inventory data for natural forests in Cambodia. The validation results showed a strong correlation ($R^2 = 0.64$) between C-MLR-estimated natural forest biomass and field-based biomass, with RMSE = 23.2 Mg/ha in deciduous forests. In high-biomass regions, such as dense evergreen forests, this model had a weaker correlation because of the high biomass and the multiple-story tree structure of evergreen forests, which caused saturation of the PALSAR signal.

Citation: Avtar R, Suzuki R, Sawada H (2014) Natural Forest Biomass Estimation Based on Plantation Information Using PALSAR Data. PLoS ONE 9(1): e86121. doi:10.1371/journal.pone.0086121

Editor: Shibu Jose, University of Missouri, United States of America

Received: September 13, 2013; **Accepted:** December 6, 2013; **Published:** January 21, 2014

Copyright: © 2014 Avtar et al. This is an open-access article distributed under the terms of the Creative Commons Attribution License, which permits unrestricted use, distribution, and reproduction in any medium, provided the original author and source are credited.

Funding: Monbukagakusho Japanese Government Fellowship to pursue research at The University of Tokyo, Japan. Global Center of Excellence programme to support field visit to Cambodia to collect ground data. Environmental Research and Technology Development Fund (F-1101) of the Ministry of Environment, Japan for preparation of manuscript. The funders had no role in study design, data collection and analysis, decision to publish, or preparation of the manuscript.

Competing Interests: The authors have declared that no competing interests exist.

* E-mail: ram.envjnu@gmail.com

Introduction

The global demand for forests and forest products is increasing because of population growth. To meet this demand, the importance of plantations has increased because they have high wood-production rates compared with natural forests [1]. Plantation forest production meets two-thirds of the global industrial roundwood demand [2]. Therefore, plantation forests are reducing the pressure on natural forests for wood and other resources, but they simultaneously pose a threat by replacing natural forests [3]. The objective of plantation forests is to produce timber and other wood products and to generate greater financial returns because of faster growth than occurs in natural forest regeneration [4]. Plantations can also be used for land rehabilitation, soil conservation, carbon sequestration, and water conservation and they can provide socio-economic benefits, minimising the poverty of local people in developing countries [5]. Different types of plantations are established for different purposes, and most are planted as monocultures [6]. These monoculture plantations, such as rubber, teak, eucalyptus, cashew, oilpalm, acacia etc., have an adverse impact on biodiversity and ecosystem services [7;8]. A recent report by Forest Resource Assessment [2] showed that plantation forests account for 7% (264 million ha) of total global forest area. During the period from 2005 to 2010, the area of planted forests increased by about 5 million ha per year worldwide. In Asia, plantation area has increased rapidly in recent

years [2]. Plantations have become an interesting topic of research under the current scenario of climate change. Carbon (C) sequestration by plantation species has become an essential concern because consideration of its effects and calculation of C-credits during climate change negotiations require estimates of C sequestration by plantation species. Therefore, examinations of plantation biophysical parameters are necessary to precisely calculate biomass. To improve sustainability, a certain ratio between plantation and natural forests is necessary. Cashew and rubber plants are the major plantation species in Cambodia [9]. Both species are exotics, and the two types of plantations differ in their canopy cover, tree size, orientation of branches, and tree distribution.

Tropical forests contain about 40% of the carbon found in terrestrial biomass [10;11;12]. The most alarming global threats in the forest sector are deforestation and forest degradation, which contribute approximately 20% of global anthropogenic CO₂ emissions [13]. Curbing deforestation through improved forest management practices could offer one of the most cost-effective methods of emission reduction [14] and could be achieved by implementing Reducing Emissions from Deforestation and forest Degradation Plus (REDD+) policies. REDD+ schemes can help to reduce emissions of CO₂ by avoiding deforestation and could also protect biodiversity and forest-derived ecosystem services. These schemes can also improve the socio-economic conditions of local and indigenous people who depend on forests for their livelihood

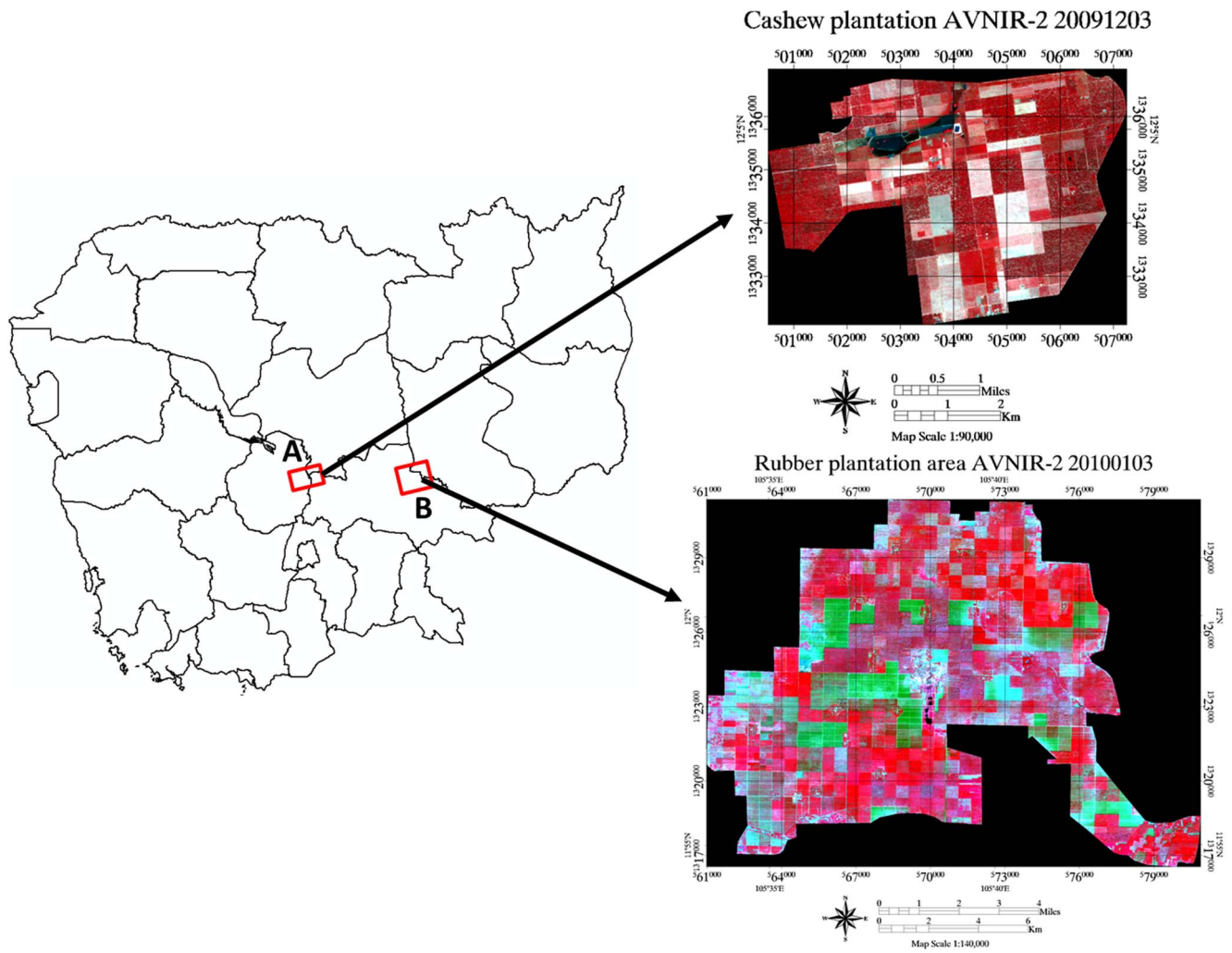


Figure 1. Location of the study area (A: Cashew plantation area, B: Rubber plantation area) AVNIR-2 data false color composite (Red:NIR, G:Red, B=Green color composite).
 doi:10.1371/journal.pone.0086121.g001

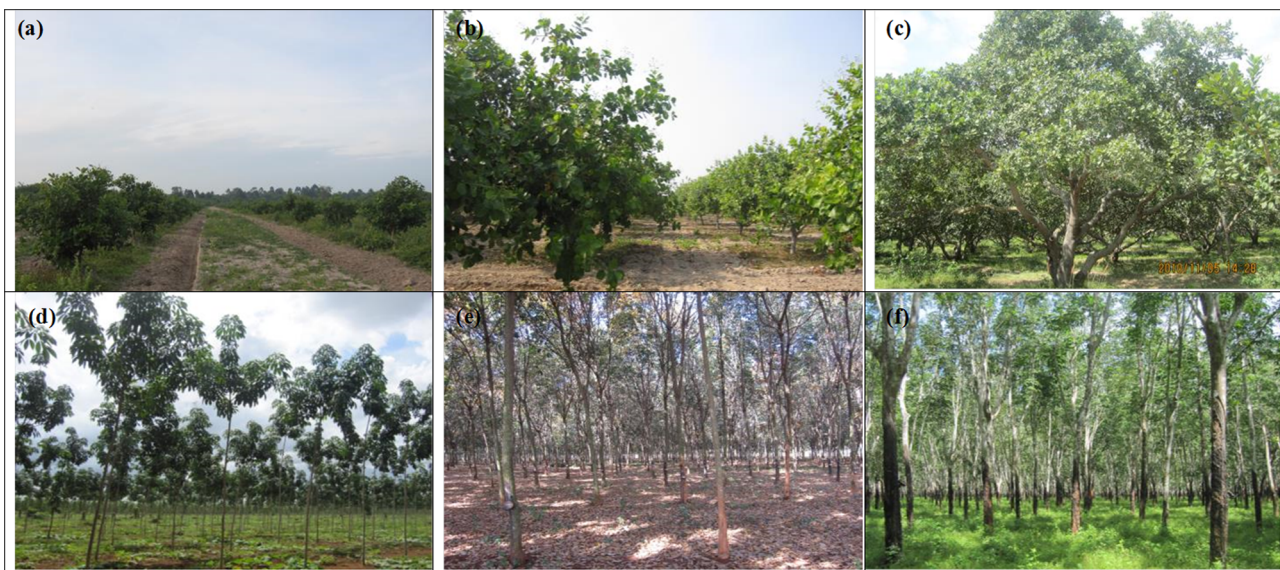


Figure 2. Cashew plantation area with different growth stages (a) juvenile, (b) young, (c) old and rubber plantation area with (d) juvenile, (e) young, (f) old growth stages.
 doi:10.1371/journal.pone.0086121.g002

Table 1. Comparison between natural and plantation forest characteristics.

	Natural Forests	Plantation Forest
1.	Multi-story (Complex structure)	Single-story (Simple structure)
2.	Multi species (Flora and fauna)	Single species (mono-culture)
3.	High biomass density (sequester more carbon)	Less biomass density (sequester less carbon)
4.	Continuous plant growth	Initial plant growth very fast
5.	Forest inventory data collection time, cost and labour intensive	Forest inventory data collection time and cost efficient
6.	Inventory data has high uncertainties	Inventory data has fewer uncertainties

doi:10.1371/journal.pone.0086121.t001

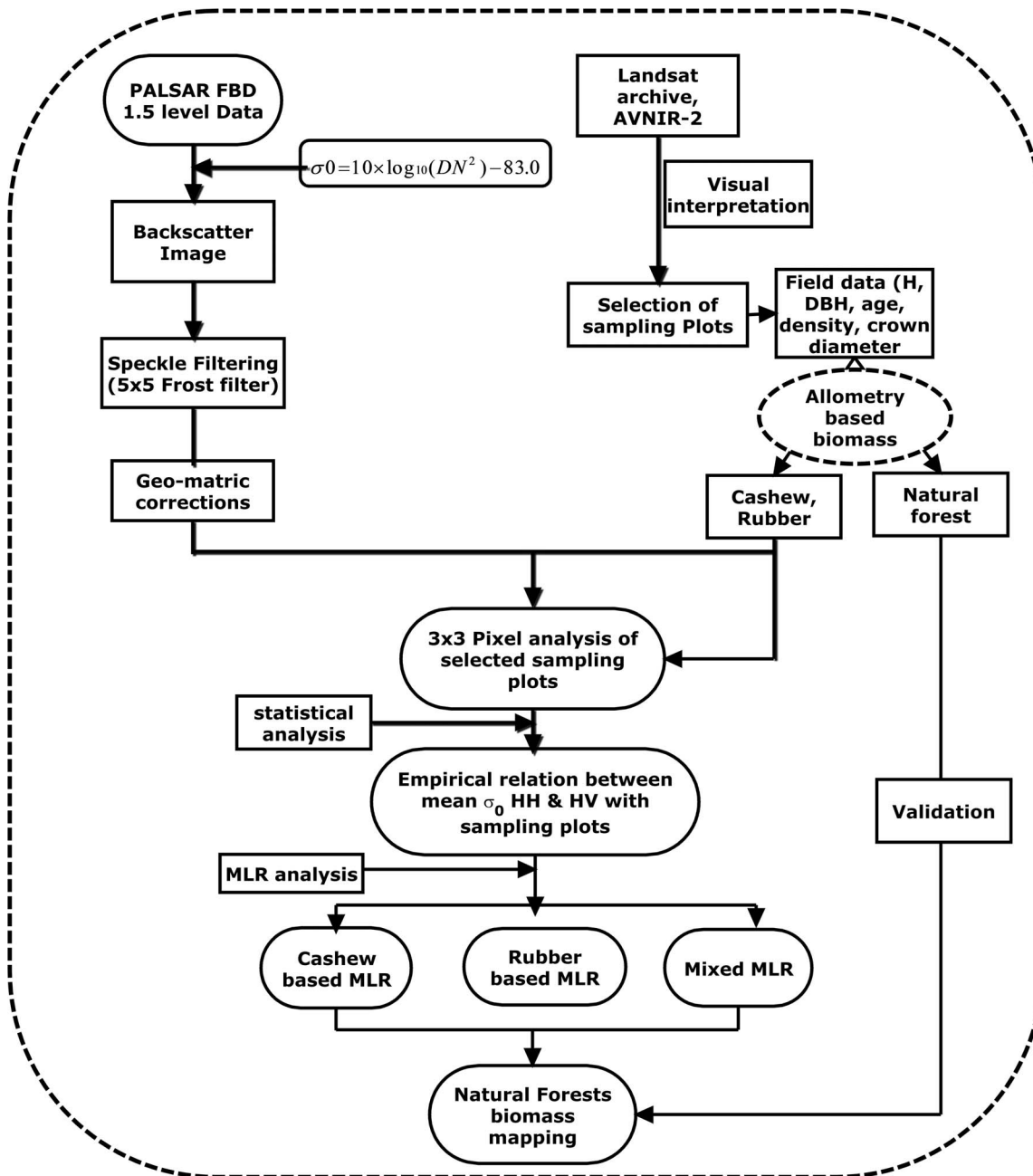


Figure 3. Flow chart of the methodology.

doi:10.1371/journal.pone.0086121.g003

Table 2. Pearson's correlation matrix of various biophysical parameters of cashew plants.

	Age (years)	Crown Dia (m)	Tree Density	Height (m)	DBH at 10 cm (cm)	DBH at 1.3 m (cm)	Biomass (Mg/ha)
Age (years)	1						
Crown Dia (m)	0.92	1					
Tree Density	-0.58	-0.64	1				
Height (m)	0.91	0.90	-0.65	1			
DBH at 10 cm (cm)	0.94	0.93	-0.64	0.93	1		
DBH at 1.3 m (cm)	0.96	0.94	-0.66	0.89	0.96	1	
Biomass (Mg/ha)	0.97	0.91	-0.53	0.88	0.95	0.97	1

doi:10.1371/journal.pone.0086121.t002

[15]. Observations of forests and their biomass distributions are the most important requirement for REDD+ [16;17;18;19]. Implementation of REDD+ policies will provide financial incentives to signatory countries that conserve and enhance their forest biomass. Because of this, precise and reliable methods are needed to estimate forest carbon stocks at national level to assess the economic benefits [20;21]. Forest carbon pools consist of trunks, branches, leaves, litter, dead wood, roots and soil carbon. However, most studies have focused on above ground biomass (AGB) because this is relatively large pool [16]. In tropical forests worldwide, about 50% of the total carbon is stored in aboveground biomass and 50% is stored in the top 1 m of the soil [22]. Satellite-based remote-sensing techniques have played a crucial role in biomass monitoring; they are more cost and time efficient than collecting forest inventory data and can provide spatial and temporal information on forest biomass distribution [23;24].

Previous studies have demonstrated that remote-sensing techniques can be used for biomass estimation using optical [25;26;27], Synthetic Aperture Radar (SAR) [28;29;30;31], and Light Detection And Ranging (LiDAR) data [32;33;34;35;36;37]. However, these techniques have several limitations; optical data saturate in low-biomass regions [38;39;40] and are not effective in tropical regions because of frequent cloud coverage [41;42]. SAR data are limited by terrain, speckle, and saturation [28;30;31]. LiDAR data are very expensive and cannot provide global coverage with plant species information [20;43]. In tropical countries, SAR is the most effective technique because it can penetrate clouds and acquire data throughout the year irrespective of cloud coverage and shadows [41].

Previous studies have shown that SAR data are dependent on various properties of the radar system (wavelength, polarisation, and incidence angle) and of the target (soil moisture, surface

roughness, vegetation structural properties, vegetation water content, and geometric properties) [44;45;46]. Forest structure and the distribution of biomass throughout the forest canopy have significant effects on radar backscatter (σ^0), which depends on the size distribution, orientation, and density of the scatterers [47]. A number of studies have been undertaken to understand the behaviour of multi-frequency (X-band, C-band, L-band, and P-band) and multi-polarisation (HH, HV, VH, and VV) SAR data with respect to forest biophysical parameters [48;49;50;51;52]. Longer wavelengths have proven more effective for biomass estimation. This study demonstrates the capability of Phased Array L-band Synthetic Aperture Radar (PALSAR) dual polarimetric (HH and HV) data for forest biomass estimation because of the high penetration of L-band SAR. The usefulness of PALSAR polarimetric data for discriminating different types of scattering from targets has been noted in previous studies [46;53;54;55].

Various studies have attempted to quantify above-ground biomass (AGB) at local to global scales [21;46;54;56;57]. However, to date, no study has used plantation information in the estimation of biomass in natural forests. In this study, we developed an empirical model based on plantation biomass and PALSAR σ^0 and applied it to natural forests in Cambodia. The primary aim of this research was to compare the biophysical parameters of cashew and rubber plants and to determine the relationship between PALSAR σ^0 and field-measured AGB. The second aim was to develop multiple linear regression (MLR) models based on a combination of plantation types (cashew, rubber, and mixed) and to compare the sensitivity of plantation-based natural forest AGB estimates using PALSAR data in Cambodia.

Study area

Both cashew and rubber plantation areas are situated in Kampong Cham Province of Cambodia. It is about 90 km from

Table 3. Pearson's correlation matrix of various biophysical parameters of rubber plants.

	Age (years)	Crown Dia. (m)	Tree density	Height (m)	DBH (cm)	Biomass (Mg/ha)
Age (years)	1					
Crown Dia. (m)	0.70	1				
Tree density	-0.48	-0.24	1			
Height (m)	0.92	0.79	-0.45	1		
DBH (cm)	0.91	0.87	-0.40	0.96	1	
Biomass (Mg/ha)	0.95	0.67	-0.35	0.95	0.92	1

doi:10.1371/journal.pone.0086121.t003

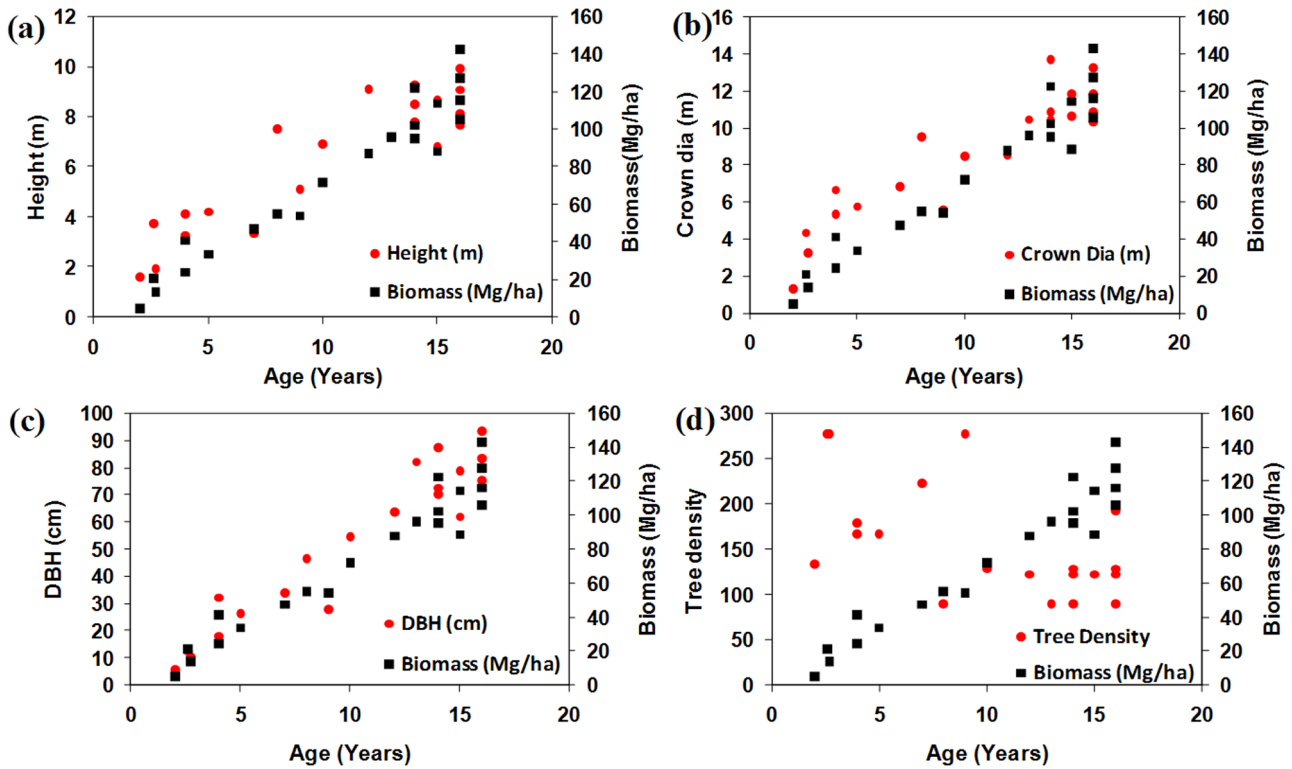


Figure 4. Relationship between age vs biomass with other biophysical parameters of cashew plants (a) height (b) crown diameter (c) DBH and (d) tree density respectively.
doi:10.1371/journal.pone.0086121.g004

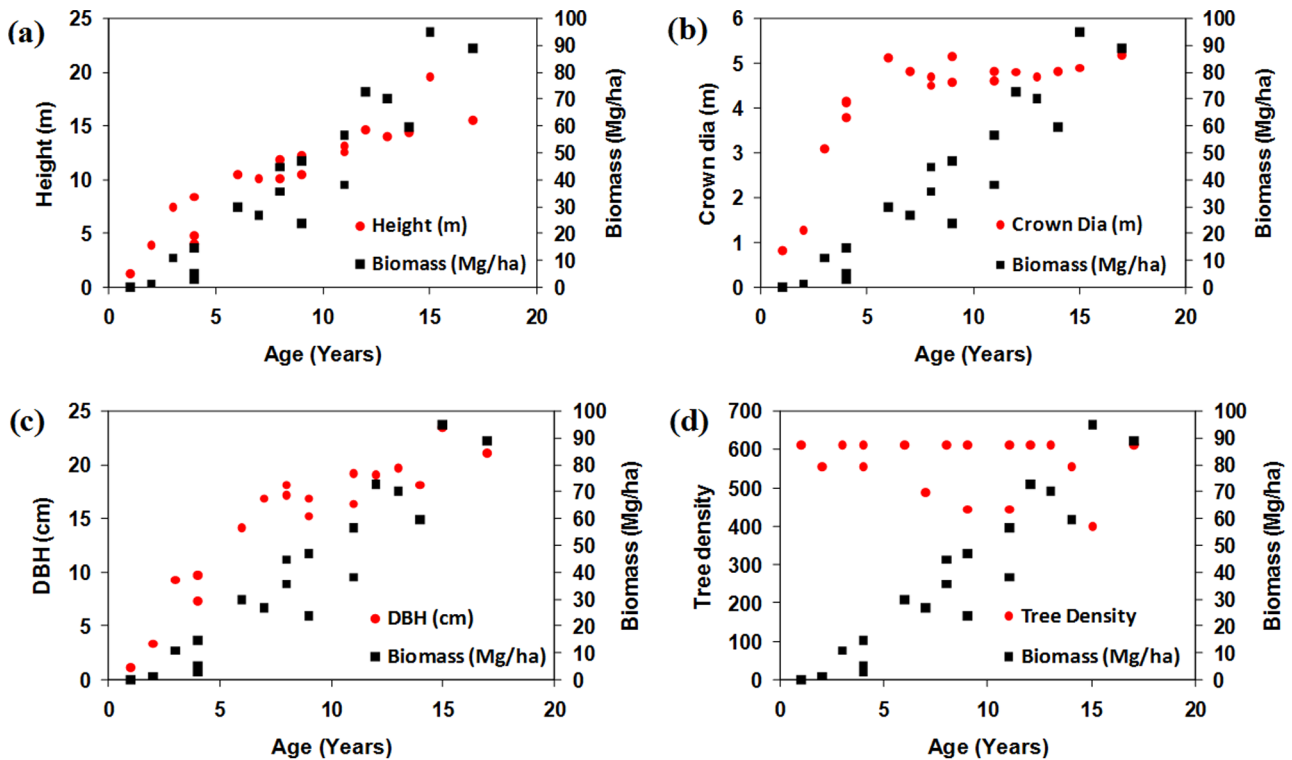


Figure 5. Relationship between age vs biomass with other biophysical parameters of rubber plants (a) height (b) crown diameter (c) DBH and (d) tree density respectively.
doi:10.1371/journal.pone.0086121.g005

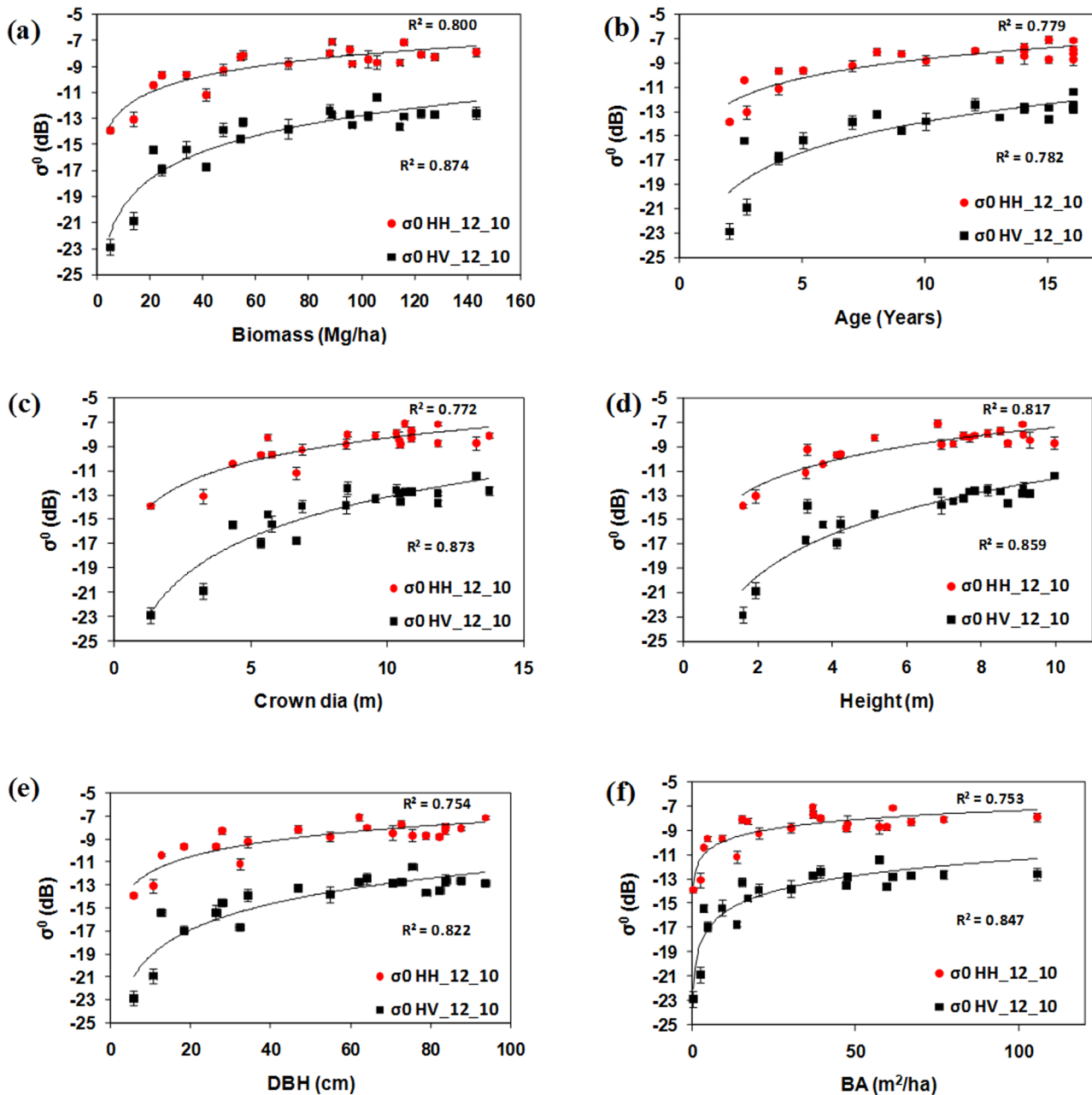


Figure 6. Relationship between PALSAR σ^0 and biophysical parameters of cashew plants (a) biomass (b) age (c) crown diameter (d) height (e) DBH and (f) basal area respectively.

doi:10.1371/journal.pone.0086121.g006

Phnom Penh and lies between $12^{\circ}2'17''N$ to $12^{\circ}6'7''N$ latitude and $104^{\circ}59'51''E$ to $105^{\circ}4'23''E$ longitude (cashew plantation area) and $12^{\circ}5'36''N$ to $12^{\circ}8'20''N$ latitude and $105^{\circ}41'9''E$ to $105^{\circ}44'11''E$ longitude (rubber plantation area). Cambodia is a tropical country with the rainy season from May to October and dry season from November to April. The minimum and maximum temperatures of the study areas are about $21^{\circ}C$ and $35^{\circ}C$, respectively. The mean annual rainfall ranges from 1500 to 1800 mm [58].

We studied the cashew and rubber plantation area managed by Agrostar private company and Chup rubber Plantation Company of Kampong Cham province respectively (Figure 1). Cashew (*Anacardium occidentale*) is an evergreen fast growing tropical tree that

grows up to 10–15 m height with a diameter at breast height (DBH) of 100 cm under favorable growing conditions [59]. Cashew plants show three stages of their growth as follows: juvenile (1–3 year), young (4–8) and mature/old (9–20). Rubber (*Hevea brasiliensis*) is a fast growing exotic species in Cambodia that grows up to 20–25 m height with a 50–60 cm DBH. Rubber is the second largest source of agricultural export after rice in Cambodia [60]. Cambodia has produced 42000 M ton of dry rubber in 2010 [13]. Rubber plant can be tapped approximately 4 to 6 years after planting. Cambodia has ideal conditions for the commercial cultivation of rubber and cashew plants [61]. Cashew and rubber plantation area are on flat areas and homogeneous spreads (same age group and same inter tree spacing) about 2,000 ha and

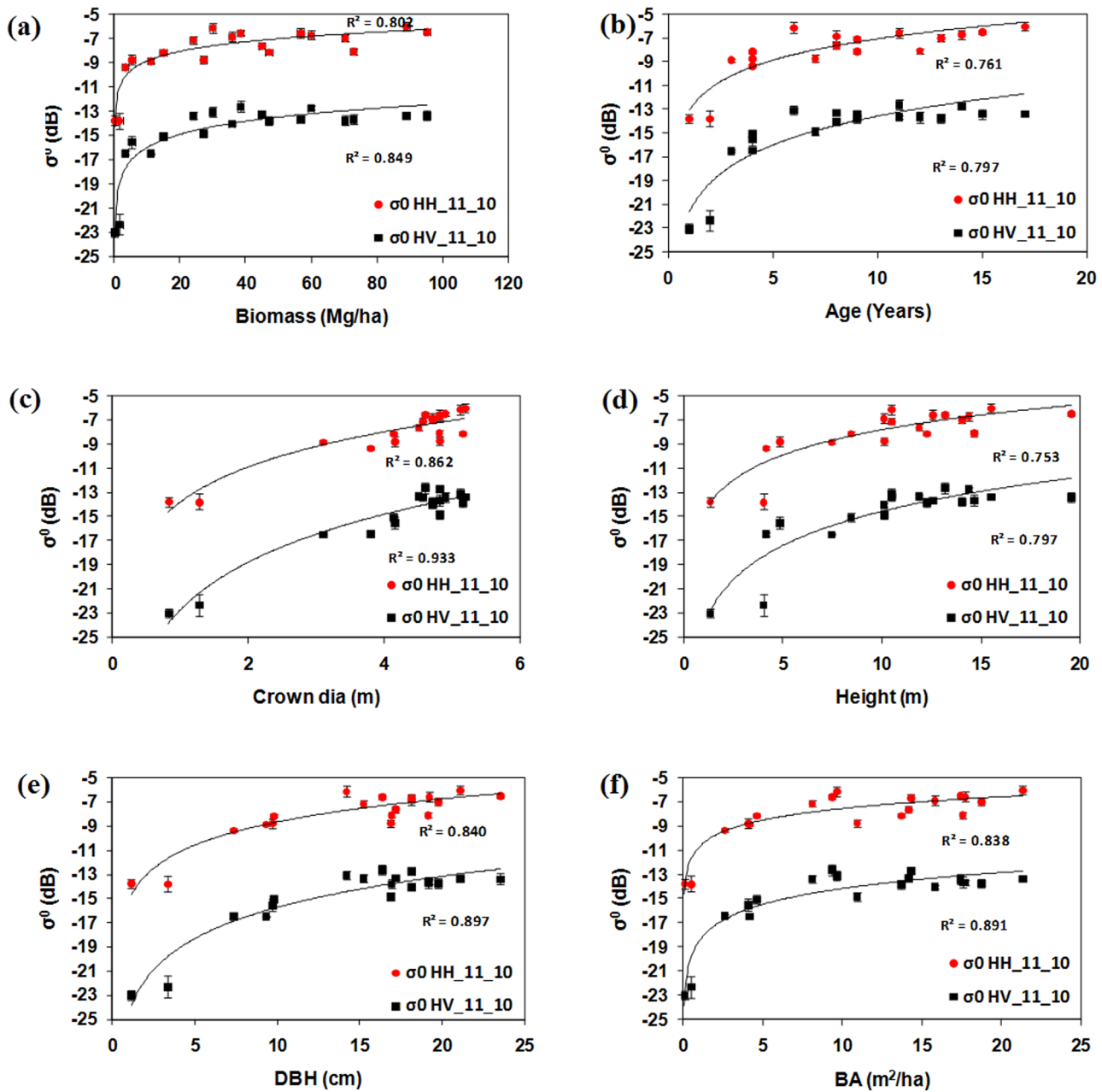


Figure 7. Relationship between PALSAR σ^0 and biophysical parameters of rubber plants (a) biomass (b) age (c) crown diameter (d) height (e) DBH and (f) basal area respectively.
doi:10.1371/journal.pone.0086121.g007

16000 ha respectively. This lack of topographic effects makes PALSAR more applicable in the measurement of plants biophysical parameters [42].

Methodology

a. Satellite data used

Analysis of satellite archive data is useful for forest inventory data collection because it can provide primary information about the starting of plantation year, extent of change in the plots and various conditions of forests [62]. Landsat archive data were downloaded from Glovis (www.glovis.usgs.gov). Three scenes of PALSAR fine beam dual (FBD) 1.5 level data acquired on

December 5th, 2010 (cashew plantation area), November 18th, 2010 (rubber plantation area) and November 1st, 2010 (natural forest area) with 34.3° off-nadir angle were used in this study [63]. PALSAR data in dry season was selected based on finding from Lucas et al. (2010) [46] to minimize effects of soil moisture on backscattering properties. Landsat archive data from 1990 to 2010 were used to establish sampling plots using visual image interpretation. Landsat archive data also provide information about the trend of cashew and rubber plantation activity and history of the starting of cashew and rubber plantation. Landsat archive shows that most of the plantation was started in between 1995 and 2000, and it was confirmed by interviewing local workers. Therefore, archive data shows the importance of

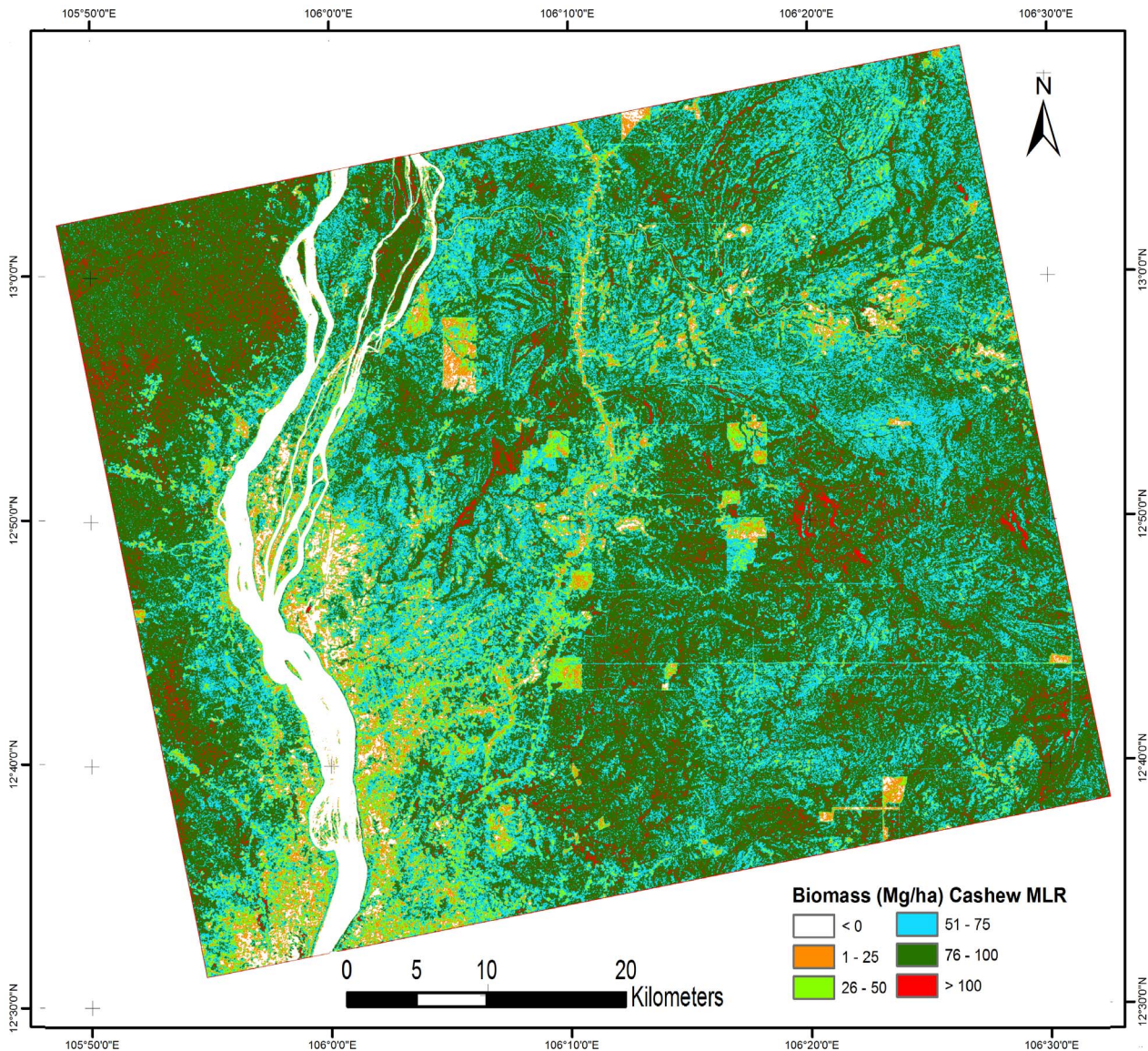


Figure 8. Natural forests biomass based on (cashew biomass MLR model 1).
doi:10.1371/journal.pone.0086121.g008

multi-temporal satellite data to know the historical information about the land use/cover pattern and their changes. Advanced Visible and Near Infrared Radiometer Type-2 (AVNIR-2) data with 10 m resolution acquired in 2010 were also used to identify the spectral signature of plantation area based on Normalized Difference Vegetation Index (NDVI) value.

b. Field data collection

Forest inventory data is useful for forest management planning and to identify the management schedules of tree stands for sustainable thinning [64]. Fieldwork was conducted in November, 2010 with the help of Forestry Administration (FA) of Cambodia, which is a government authority under the Ministry of Agriculture Forestry and Fisheries (MAFF). We also took permission from Chup Rubber Plantation Company to conduct the field survey. This field study did not involve any endangered species and no vertebrate study was conducted. A total of twenty one and nineteen sampling plots were collected to measure and estimate

specific biophysical parameters of cashew and rubber plants respectively. A stratified random sampling procedure was applied to ensure that the sampling measurements captured all possible age classes of cashew and rubber plants across the plantation area. In each sampling plot tree density, DBH, height, plantation year, and crown diameter were measured. The four corners of the plots were established in the field using Garmin Global Positioning System (GPS) 60CSx, with plot size 30×30 m to access the accuracy of PALSAR 12.5×12.5 m pixel. Eighteen sampling plots data were also collected from natural forest area during January 2011 for validation. It means, 18 sampling plots data were used to validate the natural forests biomass predicted using cashew plants based MLR model (C-MLR) and rubber plants based MLR model (R-MLR). GPS locations and photos of the plots were also collected during the field visit. Figure 2 shows the snapshot picture of the cashew and rubber plantation area with different growth stages i.e. juvenile, young and mature. Cashew plantation area (Figure 2c) shows regular spacing between two plants with multiple branches from the ground level. Rubber plantation area (Figure 2f)

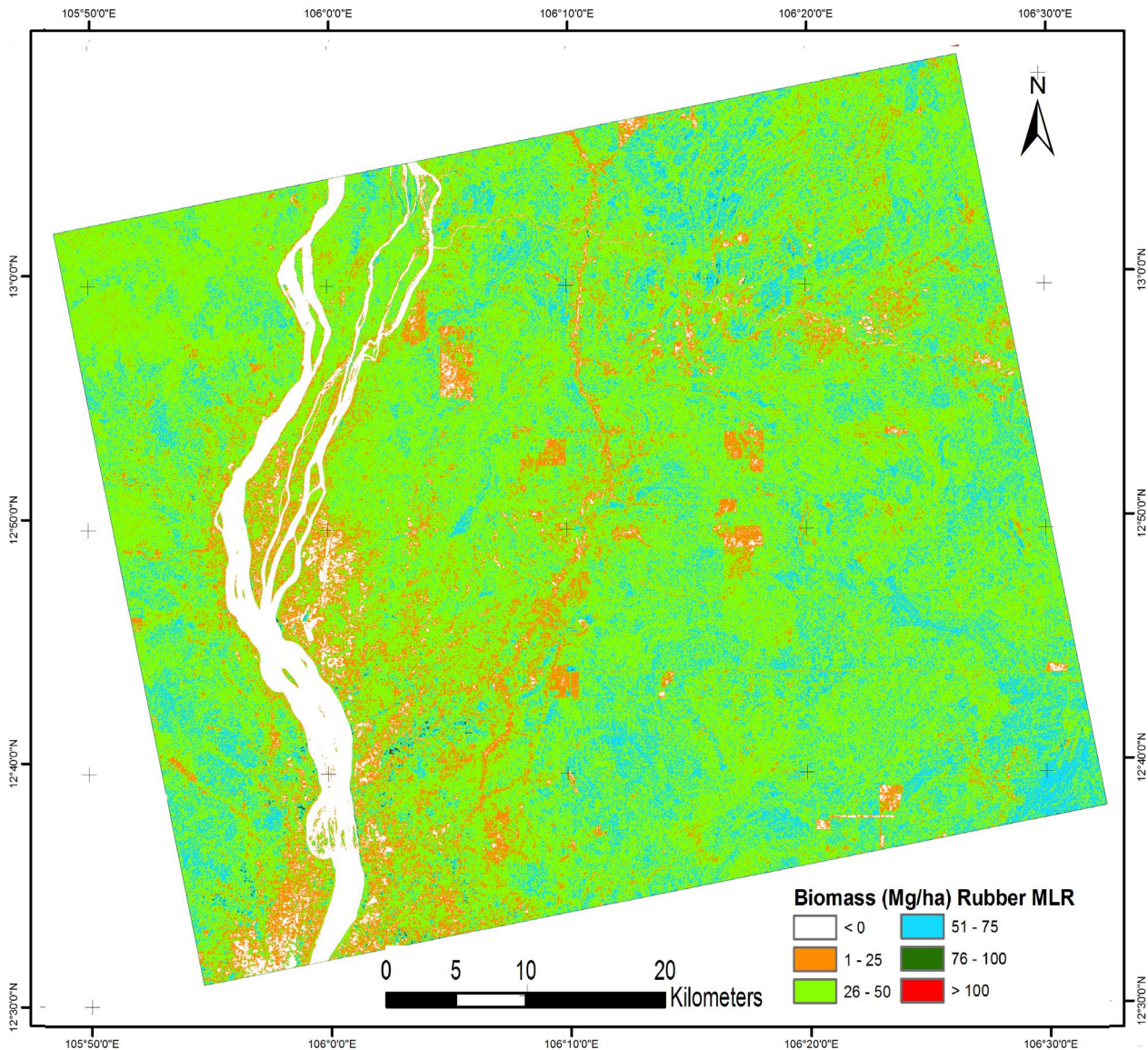


Figure 9. Natural forests biomass based on (rubber biomass MLR model 2).
 doi:10.1371/journal.pone.0086121.g009

also shows regular spacing between two plants with high tree density. Table 1 shows the comparison between the characteristics of natural forest and plantation forest. Collection of forest inventory data in plantation area is more convenient with less uncertainty compared to natural forest (based on field data collection).

The biomass of cashew plants were calculated using the following allometric equation (equation 1) [59].

$$\text{Cashew plants biomass (kg)} = 1.398 \times \text{DBH} - 0.097 \quad (1)$$

The biomass of rubber plants were calculated using the following allometric equation (equation 2) [65].

$$\log [\text{stem biomass (kg)}] = 0.866 \log D^2H - 1.255 \quad r^2 = 0.991 \quad (2)$$

$$\log [\text{branch biomass (kg)}] = 1.140 \log D^2H - 2.657 \quad r^2 = 0.878 \quad (3)$$

$$\log [\text{leaf biomass (kg)}] = 0.741 \log D^2H - 1.654 \quad r^2 = 0.922 \quad (4)$$

where, *H* and *D* represent *height* and *DBH* of rubber plant respectively. The total AGB for a tree was the sum of the stem biomass, branch biomass and leaves biomass.

The biomass of natural forest was calculated using the following allometric equation (equation 5–7) [66].

$$\text{Leaf biomass (kg)} = 173 \times BA^{0.938} \quad (5)$$

$$\text{Branch biomass (kg)} = 0.217 \times BA^{1.26} \times D^{1.48} \quad (6)$$

$$\text{Stem biomass (kg)} = 2.69 \times BA^{1.29} \times D^{1.35} \quad (7)$$

where, *BA* and *D* represents basal area (m^2) and DBH of the tree respectively. The total AGB for a tree was the summation of the stem biomass, branch biomass and leaves biomass.

c. Satellite data processing

AVNIR-2 data and Landsat data were used for selection of sampling sites. PALSAR FBD data were processed for converting digital number (DN) to σ^0 . The backscattering coefficient was calculated using the following equation [67].

$$\sigma^0 = 10 \times \log_{10} (DN^2) + CF \quad (8)$$

Where, CF is the calibration factor and its value for PALSAR FBD 1.5 L data is -83 because it was acquired after 9th January, 2009. The PALSAR data were co-registered with AVNIR-2 data

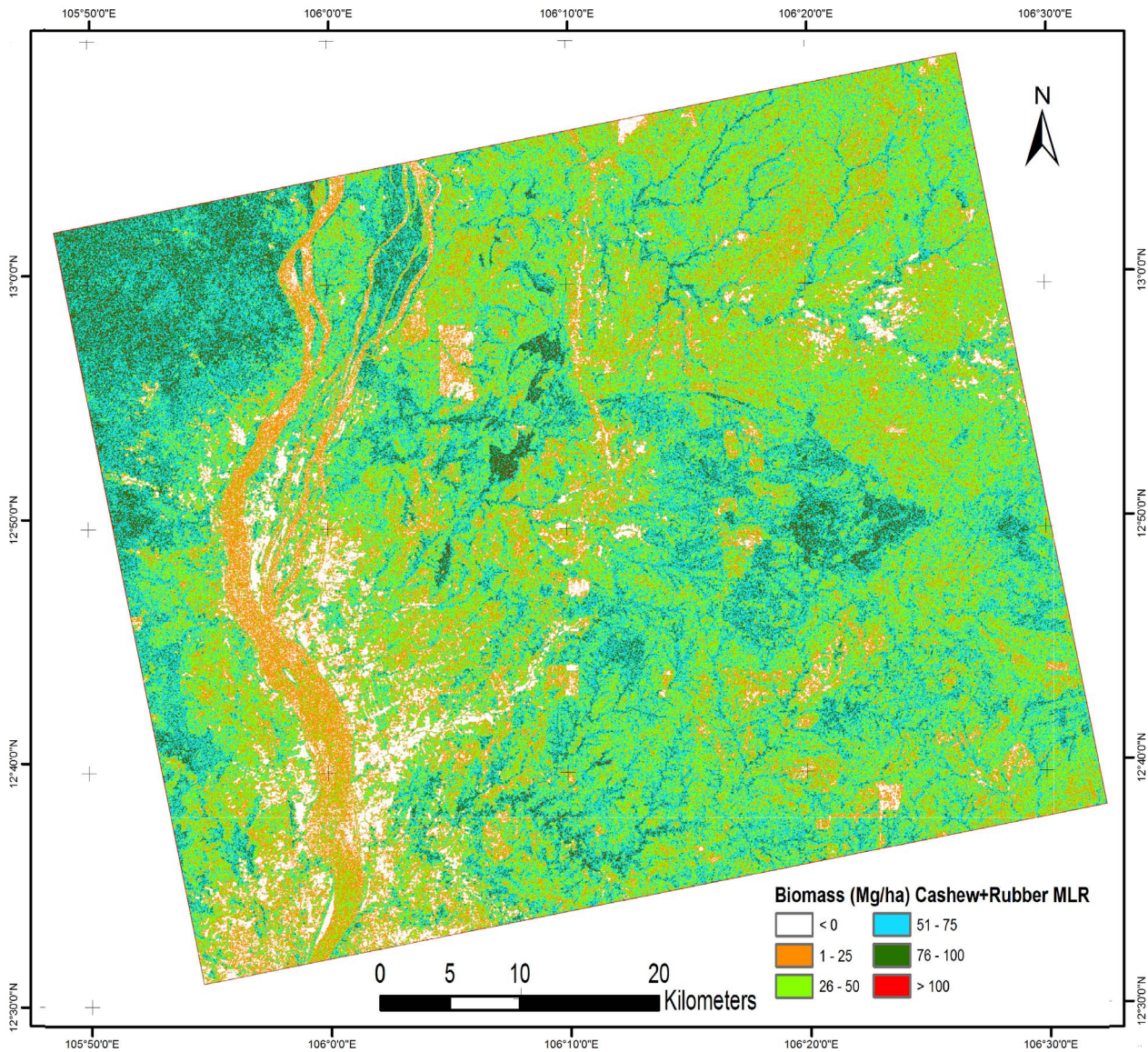


Figure 10. Natural forests biomass based on (cashew + rubber biomass MLR model 3).
doi:10.1371/journal.pone.0086121.g010

based on field collected ground control points (GCPs). Later the data were filtered with window size of 5×5 to reduce speckle noise [68]. We have considered the climatic conditions of the area during the analysis of PALSAR data to minimize climatic effects.

d. Statistical Analysis

The mean σ^0 was calculated for each sampling plots with 3×3 pixels size. We used 3×3 pixels window size to minimize the positional inaccuracies of GPS and geo-coding. The relationships between σ^0 and biophysical parameters were analyzed using logarithmic equation because of the backscattering value of PALSAR is in logarithmic scale. Correlation analysis and

Table 4. MLR model based on cashew and rubber plants biomass.

No.	Plantation type	PALSAR Polarization	R ²	R ² Adj	Regression Model No.
1	Cashew	HH, HV	0.63	0.59	$Y(\text{biomass}) = 242.9 + 3.1 \times \sigma^0_{HH} + 9.7 \times \sigma^0_{HV}$
2	Rubber	HH, HV	0.43	0.36	$Y(\text{biomass}) = 108.6 + 9.1 \times \sigma^0_{HH} - 0.25 \times \sigma^0_{HV}$
3	Cashew + Rubber (Mixed)	HH, HV	0.54	0.52	$Y(\text{biomass}) = 206.1 - 12.7 \times \sigma^0_{HH} + 17.6 \times \sigma^0_{HV}$

doi:10.1371/journal.pone.0086121.t004

Table 5. Percentage of biomass distribution for different biomass map.

No.	Biomass class (Mg/ha)	Cashew based MLR (% area) (Figure 8)	Rubber based MLR (% area) (Figure 9)	Cashew + Rubber based MLR (% area) (Figure 10)	Cashew - Rubber difference biomass (% area) (Figure 11)
1	0	5.54%	5.55%	6.67%	8.12%
2	1-25	3.92%	10.19%	16.66%	21.29%
3	26-50	8.65%	65.87%	37.91%	61.01%
4	51-75	28.46%	18.12%	30.16%	9.45%
5	76-100	49.38%	0.22%	8.01%	0.10%
6	>100	4.04%	0.04%	0.59%	0.03%
7	Total	100%	100%	100%	100%

doi:10.1371/journal.pone.0086121.t005

Multi-linear regression (MLR) model approach have been applied. Field based biophysical parameters and PALSAR backscattering in HH, HV mode were used in MLR approach. MLR approach

has also been used by previous researcher and good results have been achieved in their studies [46;47;50;51;54;65;69;70]. MLR analysis using the stepwise forward method was conducted relating

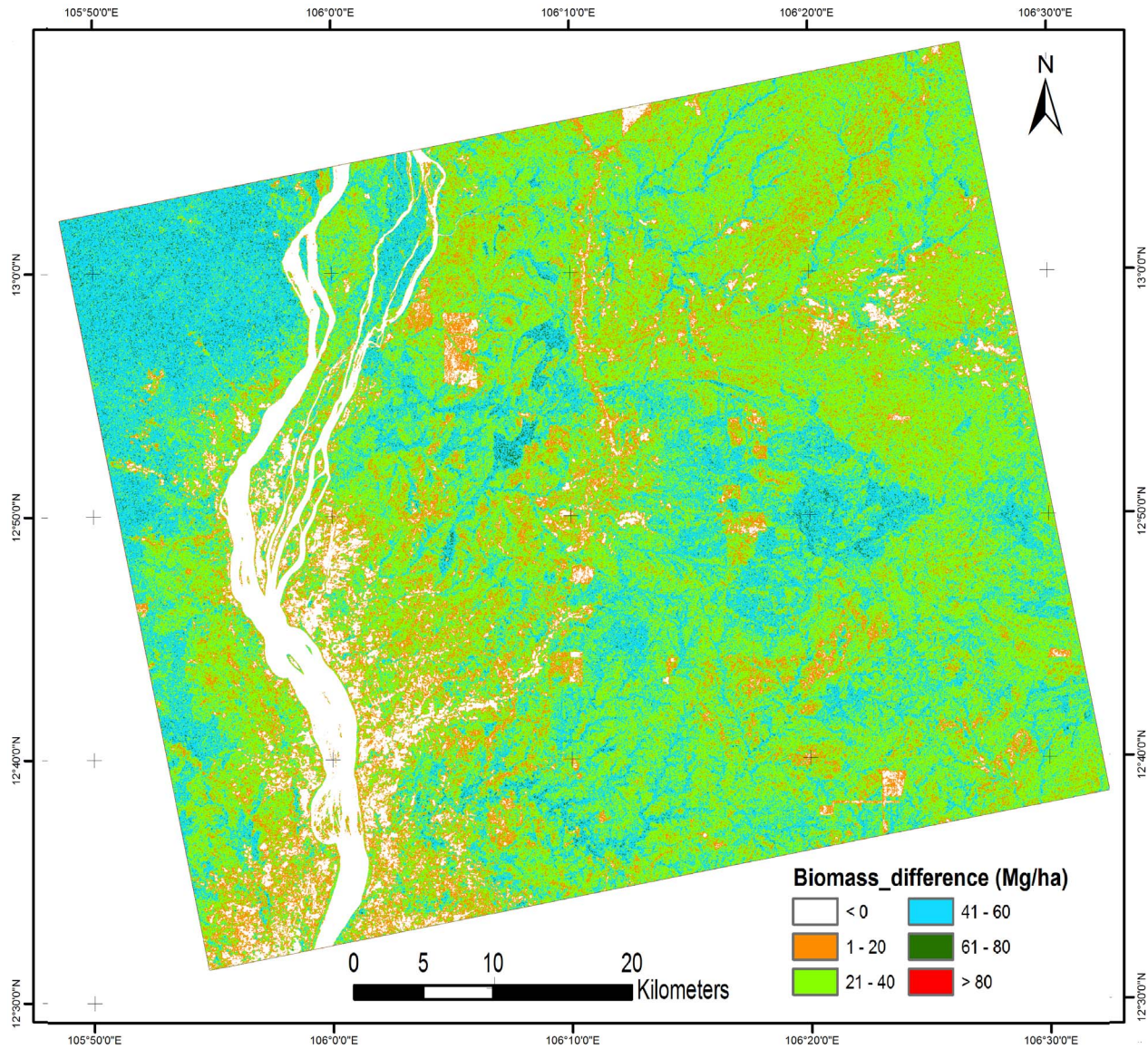


Figure 11. Biomass difference map (MLR model 1 - MLR model 2).
doi:10.1371/journal.pone.0086121.g011

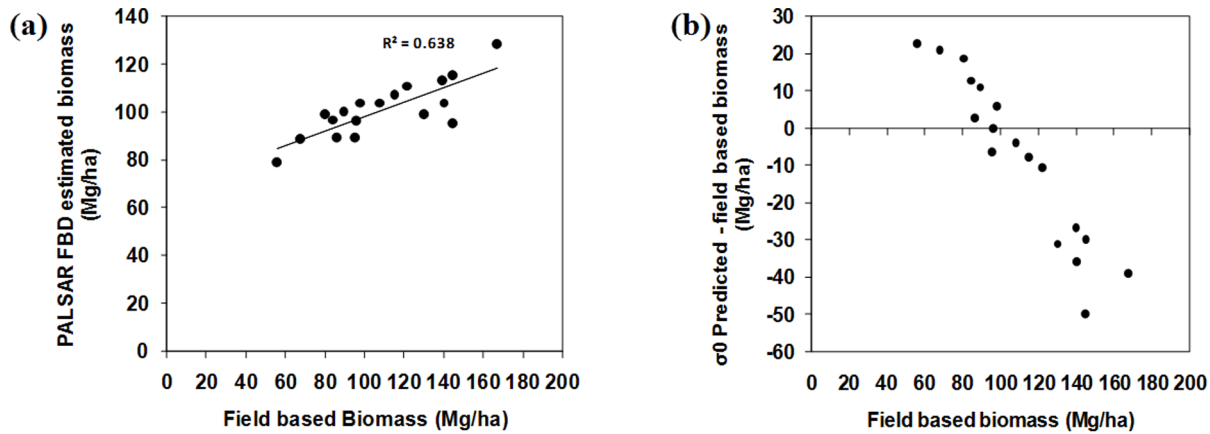


Figure 12. Validation results of biomass map (a) Relationship between PALSAR predicted natural forests biomass plotted against field measured biomass of natural forests (b) the error in PALSAR predicted natural forests biomass plotted against field measured biomass of natural forests.

doi:10.1371/journal.pone.0086121.g012

the σ^0 of PALSAR to corresponding field calculated biomass [67;71]. We have generated three MLR models using cashew (C-MLR), rubber (R-MLR) and mixed (M-MLR) plantation types. Here mixed means joining of the plots from pure cashew and pure rubber plantations. These models have been applied to the PALSAR data to estimate biomass of natural forests. Finally validation was used to evaluate the accuracy of the model by comparing PALSAR estimated AGB to the field derived AGB. Figure 3 illustrates the flow chart of methodology adopted in this study.

Results and Discussion

a. Comparison of cashew and rubber plant biophysical parameters

A correlation matrix among the various biophysical parameters of cashew and rubber plants is summarised in Tables 2 and 3. The correlation matrix shows that all respective biophysical parameters are well correlated except tree density. Basic information on planted clones, area of plantation, and age of trees was obtained from plantation owners and workers with the help of an interpreter. Information about the plantation history and agro-forestry practices was also collected [72;73].

Statistical analyses were conducted to compare biophysical parameters of cashew and rubber plants. Figures 4 (a, b, c, d) and 5 (a, b, c, d) show relationships for height, crown diameter, diameter at breast height (DBH), and tree density with respect to age *vs.* biomass of cashew and rubber plants. Biophysical parameters of cashew plants showed positive relationship with plant age and biomass (Figure 4a, b, c), with the exception of tree density (Figure 4d). Biophysical parameters of rubber plants also showed positive relationship with plant growth and biomass (Figure 5a, c), except for crown diameter and tree density (Figure 5b, d). Cashew plants had greater biomass, DBH, and crown diameter compared with rubber plants at their mature stage. Tree density is a conditional parameter and depends on the species of the seedlings used. Variability in tree density in cashew plants arises because diseases and insects affect or kill trees that do not get enough light due to shade from neighbouring trees. However, in the case of rubber plants, tree density as a function of age is relatively stable. Rubber plants reach maturity after 4 years of growth and provide commercial yield. Field data also show that rubber plants do not show significant increases in crown diameter after approximately 6

years of growth (Figure 5d), whereas cashew plants show regular increases in crown diameter.

PALSAR data with HH and HV polarisation were analysed for their relationships with the cashew and rubber plant biophysical parameters. High penetration of L-band SAR showed a positive relationship with cashew and rubber plant biophysical parameters. Figures 6 (a, b, c, d, e, f) and 7 (a, b, c, d, e, f) show relationships between PALSAR backscattering and ground-based measurements of biophysical parameters of cashew and rubber plants. Although both HH and HV polarisation showed positive relationships with field-based data, the sensitivity of σ^0 HV was higher than that of σ^0 HH in both plantation types because of an increase in the volume of scattering with the growth of cashew and rubber plants. Low backscattering and high variation were seen at juvenile stages in cashew and rubber plants, mainly due to high growth rates during juvenile stages. After a certain amount of growth (4–5 years), cashew and rubber plants reached maturity and showed high backscattering. Because of fast growth during juvenile stages, the gaps between plants decreased considerably within 3 to 4 years after planting. During juvenile stages, plants had smaller leaves and fewer branches that caused less scattering, resulting in low σ^0 HV. The gaps between canopies as growth proceeded gradually decreased, making the surface less visible. High backscattering and low variation were observed with mature cashew and rubber plants because of their homogeneous canopies. This increase in σ^0 was mainly caused by growth in the plants' biophysical parameters.

Backscattering coefficient of HV polarization showed saturation around 100 Mg/ha biomass for cashew and 50 Mg/ha for rubber plants. Saturation of the PALSAR signal occurred after 13 years of growth in cashew plants. However, in rubber plants, saturation at 50 Mg/ha was because of saturation in crown cover. As in rubber plants, there was no significant increase in crown diameter after 6 years of growth. The rubber plant has a simple and symmetrical canopy, with homogeneous crown cover that becomes stable after 6 years of growth, whereas cashew plants show branching from the ground level, with a large crown diameter that increases with age and overlaps with adjacent trees. Therefore, cashew plants cause higher scattering volume in mature stages than rubber plants do. In this study, we observed that growth in the crown size of rubber and cashew plants was the main factor contributing to the volume of scattering [51;50]. We observed high R^2 values of σ^0 HH and HV with biophysical parameters of cashew and rubber plants.

However, σ^0 HV showed stronger correlations than σ^0 HH with biophysical parameters in both plants previous studies also noticed strong correlation between HV polarization and plants biophysical parameters [50], [51].

c. MLR model generation and application in a natural forest area

Based on the above observations, three MLR models were created: Model 1 (cashew plant-based biomass), Model 2 (rubber plant-based biomass), and Model 3 (mixture of cashew and rubber plant-based biomass). Table 4 shows all three models with their R^2 value. Model 1 had a high R^2 value compared with models 2 and 3. These models were applied to PALSAR data from a natural forest area to predict tree biomass. The results of the AGB estimation for the natural forest are shown in Figures 8, 9 and 10 using models 1, 2, and 3, respectively. Table 5 shows the biomass distribution of the PALSAR-derived biomass map. From figure 8, it can be seen that throughout the deciduous forest, the amount of AGB was generally 51–100 Mg/ha. In some areas near a river, the AGB value was very low (1–25 Mg/ha) because most of the area was covered by agricultural land, where rice cultivation is common in the sampling season. In figure 8, the evergreen forest also shows an AGB value around 100 Mg/ha due to saturation of the PALSAR signal. Therefore, the application of model 1 in low-biomass regions, such as deciduous forests, is useful, but in high-biomass regions, such as evergreen forests, it shows saturation of the PALSAR signal. Figure 9 shows most of the deciduous forest area, where the amount of biomass varies from 26 to 50 Mg/ha. Even high-biomass regions such as evergreen forests show low-biomass values (50–75 Mg/ha). Thus, biomass prediction using model 2, which is based on the rubber plant, is not suitable. Figure 10 shows that in most of the deciduous area, the amount of biomass varies from 26 to 75 Mg/ha. The biomass prediction from model 3, which is based on both rubber and cashew plants, also resulted in underestimation and is not suitable for biomass prediction. Therefore, based on the regression results, we concluded that the methodological approach adopted in this study could be applied to estimate biomass in low-biomass regions such as deciduous forests. The results obtained from MLR model 1, which used cashew plant-based information, is the most promising among the models examined.

Figure 11 shows a biomass difference map comparing models 1 and 2. This map shows that the biomass in most of the area differed by 26–50 Mg/ha. We have observed that cashew plants show similar biomass patterns to deciduous forests in Cambodia. This model can be used to obtain a general idea of the biomass distribution. The plantation-based natural forest biomass estimation cannot provide accurate values in high-biomass regions because of saturation of the PALSAR signal. However, this technique is cost and time effective because the collection of forest inventory parameters in plantation areas is more convenient and has lower uncertainty compared with natural forests (Table 1). To overcome the saturation problem in high-biomass regions (100 Mg/ha), we need to examine P-band SAR or DESDynl satellites in the future [74]

References

- Carle J, Holmgren P (2008) Wood from planted forests: A global outlook 20052030 *Forest Products Journal*, 58(12): 6–18
- FRA, 2010 Global forest resource assessment country report Cambodia Rome
- Evans J, Turnbull J (2004) *Plantation Forestry in the Tropics* (3rd ed), Oxford University Press, Oxford
- Lamb D (2011) *Regreening the bare hills: Tropical forest restoration in the Asia-Pacific region*, Springer, New York
- Stephens SS, Wanger MR (2007) Forest plantation and biodiversity: A fresh perspective *Journal of Forestry*, 105 (6): 307–313
- Evans J (2009) *Forests uses, impacts & sustainability*, FAO, MPG Books group, UK
- Bunker DE, DeClerck F, Bradford JC, Colwell RK, Perfecto I, et al. (2005) Species loss and aboveground carbon storage in a Tropical Forest Science 310: 1029–1031

d. Validation

Figure 12 (a, b) shows validation results for model 1-predicted (Figure 8) PALSAR-derived biomass with field measured biomass in natural forests. The sensitivity of PALSAR predicted AGB decreases as biomass increase because of saturation of the PALSAR signal. There was a significant correlation between model estimates and field measured biomass, $R^2 = 0.64$. The overall root mean square error (RMSE) for the validation result was 23.2 Mg/ha. High variation in the error was present in high-biomass regions, i.e. where the biomass was greater than 100 Mg/ha (Figure 12b). Most of the high-biomass region showed underestimation by model 1.

Conclusions

The relationships between biophysical parameters and PALSAR σ^0 was investigated in cashew and rubber plantation areas. σ^0 HV showed a higher positive correlation with field-based biomass data than did σ^0 HH. Cashew plants showed saturation at 100 Mg/ha, whereas rubber plants showed saturation at 50 Mg/ha. In this study, we found that crown diameter was the main contributing factor to the volume of scattering. This study demonstrates that PALSAR data can be used to differentiate canopy structure. The development of plantation-based biomass-estimation models provides a new method to derive biomass in a cost-effective and timely way. The validation results showed a strong correlation between model estimations and field-based measurements ($R^2 = 0.64$) with RMSE = 23.2 Mg/ha in deciduous forests in Cambodia. We can use the generated biomass map to obtain a general idea of the biomass distribution because in high-biomass regions, this model becomes saturated. The advantage of this method is that it minimises cost, time, and labour during the collection of forest inventory data. The collection of inventory parameters is very easy and convenient, and it does not disturb the local ecosystem in plantation areas compared with natural forest areas (based on field experience). Further investigation into the use of full polarimetric PALSAR data with Cloude-Potteir, Freeman-Durden and Yamaguchi 4 component based decomposition parameters could help us to quantify and understand the scattering mechanisms from plantations and natural forests and their roles in forest biomass estimation.

Acknowledgments

The authors are highly thankful to the Forestry Administration (FA), Cambodia and Forestry and Forest Products Research Institute (FFPRI), Japan for their cooperation during the field data collection.

Author Contributions

Conceived and designed the experiments: RA. Performed the experiments: RA. Analyzed the data: RA. Contributed reagents/materials/analysis tools: RA RS HS. Wrote the paper: RA.

8. Lal R (2008) Carbon sequestration *Philosophical Transactions of the Royal Society B*, 363: 815–830
9. MAFF (2010), Ministry of agriculture, forestry and fisheries report
10. Dixon RK, Brown S, Houghton RA, Solomon AM, Trexler MC, et al. (1994) Carbon pools and flux of global forest ecosystems *Science* 263: 185–190
11. Phillips OL, Malhi Y, Higuchi N, Laurance WF, Nunez PV, et al. (1998) Changes in the carbon balance of tropical forests: evidence from long-term plots *Science* 282: 439–442
12. Watson RT, Noble IR, Bolin B, Ravindranath NH, Verardo DJ, et al. (eds) (2000) Land use, land-use change, and forestry A special report of IPCC Cambridge University Press, Cambridge
13. Van der Werf GR, Morton DC, Defries RS, Olivier JGJ, Kasibhatla PS, et al. (2009), CO₂ emissions from forest loss, *Nature Geoscience*. 2: 737–739
14. Putz FE, Zuidema PA, Pinard MA, Boot RGA, Sayer JA, et al. (2008) Improved tropical forest management for carbon retention, *PLoS Biol*, 6, 7 e166: 1368–1369
15. Dudley RG (2010) A little REDD model to quickly compare possible baseline and policy scenarios for reducing emissions from deforestation and forest degradation Mitigation and Adaptation Strategies for Global Change, 15: 53–69.
16. Avtar R, Suzuki R, Takeuchi W, Sawada H (2013) PALSAR 50m mosaic based national level biomass estimation for REDD+ policies implementation *PLOSone*, 8, 10, e74807.
17. Avtar R, Sawada H, Kumar P (2013) Role of remote sensing and community forestry to manage forests for the effective implementation of REDD+ mechanism: A case study on Cambodia Environment, Development and Sustainability, DOI: 10.1007/s10668-013-9448-y
18. Avtar R, Sawada H (2012) Use of DEMs data to monitor height changes due to deforestation *Arabian Journal of Geosciences*, DOI: 10.1007/s12517-012-0768-2
19. Avtar R, Sawada H, Takeuchi W, Singh G (2012) Characterization of Forests and Deforestation in Cambodia Using ALOS/PALSAR Observation *Geocarto International*, 27(2): 119–137
20. Gibbs HK, Brown S, Niles JO, Foley JA (2007) Monitoring and estimating tropical forest carbon stocks: making REDD a reality *Environmental Research Letters*, 2, 045023, 13
21. Saatchi SS, Harris NL, Brown S, Lefsky M, Edward TA, et al. (2011) Benchmark map of forest carbon stocks in tropical regions across three continents *PNAS* 14, 108 (24): 9899–9904.
22. Rosenqvist A, Milne A, Lucas R, Imhoff M, Dobson C (2003) A review of remote sensing technology in support of the Kyoto Protocol *Environmental Science and Policy*, 6: 441–455.
23. DeFries R, Achard F, Brown S, Herold M, Murdiyoso D, et al. (2007) Earth observations for estimating greenhouse gas emissions from deforestation in developing countries *Environmental Science and Policy*, 10: 385–394
24. Angelsen A, Brown S, Loisel C, Peskett L, Streck C, et al. (2009) Reducing Emissions from Deforestation and Forest Degradation (REDD): an options assessment report Washington, DC: Meridian Institute
25. Sader SA, Waide RB, Lawrence WT, Joyce AT (1989) Tropical forest biomass and successional age class relationships to a vegetation index derived from Landsat TM data *Remote Sensing of Environment*, 28: 143–156
26. Steining MK (2000) Satellite estimation of tropical secondary forest aboveground biomass: Data from Brazil and Bolivia *International Journal of Remote Sensing*, 21, 6: 1139–1157
27. Foody GM, Boyd DS, Cutler MEJ (2003) Predictive relations of tropical forest biomass from Landsat TM data and their transferability between regions *Remote Sensing of Environment*, 85, 4: 463–474
28. Imhoff ML (1995) Radar backscatter and biomass saturation-Ramifications for global biomass inventory *IEEE Transactions on Geoscience and Remote Sensing*, 33(2): 511–518
29. Luckman A, Baker J, Kuplich TM, Yanasse CDF, Frery AC (1997) A study of the relationship between radar backscatter and regenerating tropical forest biomass for spaceborne SAR instruments *Remote Sensing of Environment*, 60(1): 1–13.
30. Kasischke ES, Melack J M, Dobson MC (1997) The use of imaging radars for ecological applications- A review *Remote Sensing of Environment*, 59(2): 141–156.
31. Santos JR, Freitas CC, Araujo LS, Dutra LV, Mura JC, et al. (2003) Airborne P-band SAR applied to the aboveground biomass studies in the Brazilian tropical rainforest *Remote Sensing of Environment*, 87(4): 482–493.
32. Nilsson M (1996) Estimation of tree heights and stand volume using an airborne lidar system *Remote Sensing of Environment*, 56, 1: 1–7.
33. Naesset E (1997) Determination of mean tree height of forest stands using airborne laser scanner data *ISPRS Journal of Photogrammetry and Remote Sensing*, 52: 49–56.
34. Lefsky MA, Cohen WB, Harding DJ, Parker GG, Acker SA, et al. (2002) Lidar remote sensing of above-ground biomass in three biomes *Global Ecology and Biogeography*, 11, 5: 393–399.
35. Drake JB, Dubayah RO, Clark DB, Knox RG, Blair JB, et al. (2002) Estimation of tropical forest structural characteristics using large-footprint Lidar *Remote Sensing of Environment*, 79: 305–319.
36. Drake JB, Knox RG, Dubayah RO, Clark DB, Condit R, et al. (2003) Above-ground biomass estimation in closed canopy neotropical forests using lidar remote sensing: Factors affecting the generality of relationships *Global Ecology and Biogeography*, 12: 147–159.
37. Clark ML, Clark DB, Roberts DA (2004) Small-footprint Lidar estimation of subcanopy elevation and tree height in a tropical rain forest landscape *Remote Sensing of Environment*, 91, 1: 68–89.
38. Fassnacht KS, Gower ST, MacKenzie MD, Nordheim EV, Lillesand TM (1997) Estimating the leaf area index of North Central Wisconsin forests using the landsat thematic mapper *Remote Sensing of Environment*, 61: 229–245.
39. Anderson MC, Neale CMU, Li F, Norman JM, Kustas WP, et al. (2004) Upscaling ground observations of vegetation water content, canopy height, and leaf area index during SMEX02 using aircraft and Landsat imagery *Remote Sensing of Environment*, 92: 447–464.
40. Wang Q, Adiku S, Tenhunen J, Granier A (2005) On the relationship of NDVI with leaf area index in a deciduous forest site *Remote Sensing of Environment*, 94: 244–255.
41. Lu D (2006) The potential and challenge of remote sensing-based biomass estimation, *International Journal of Remote Sensing*, 27, 7: 1297–1328.
42. Avtar R, Takeuchi W, Sawada H (2013) Monitoring of biophysical parameters of cashew plants in Cambodia using ALOS/PALSAR data *Environmental Monitoring and Assessment*, 185: 2013–2037.
43. Cohn SA, Mayor SD, Grund CJ, Weckwerth TM, Senff C (1998) The Lidars in flat terrain (LIFT) experiment *Bulletin of American Meteorological Society*, 79, 7: 1329–1343.
44. Ulaby FT, Moore RK, Fung AK (1982) *Microwave Remote Sensing: Active and Passive Volume 2: Radar Remote Sensing and Surface Scattering and Emission Theory*, Addison- Wesley, Advanced Book Program: Reading, Massachusetts, 609.
45. Santoro M, Eriksson L, Askne IJ, Schmillius C (2006) Assessment of standwise stem volume retrieval in boreal forest from JERS-1 L-band SAR backscatter *International Journal of Remote Sensing*, 27, 16: 3425–3454.
46. Lucas R, Armston J, Fairfax R, Fensham R, Accad A (2010) An Evaluation of the ALOS PALSAR L-Band Backscatter—Above Ground Biomass Relationship Queensland, Australia: Impacts of Surface Moisture Condition and Vegetation Structure Selected Topics in Applied Earth Observations and Remote Sensing, *IEEE Journal of* 3, 4 :576–593.
47. Ribbes F, Toan TL, Bruniquel J, Floury N, Syussi N, et al. (1997) Forest mapping in tropical region using multitemporal and interferometric ERS-1/2 data In: *Proceedings of the 3rd ERS symposium on space at the service of our environment*, Florence, Italy, Estec, Noordwijk, The Netherlands: 351–356 ESA SP-414.
48. Rauste Y, Häme T, Pulliainen J, Heiska K, Hallikainen M (1994) Radar-based forest biomass estimation *Int J Remote Sens* 15: 2797–2808.
49. Ranson KJ, Sun G (1997) An evaluation of AIRSAR and SIRC/X-SAR images for mapping northern forests attributes in Maine, USA *Remote Sens Environ* 59: 203–22.
50. Dobson MC, Ulaby FT, Le Toan T, Beaudoin A, Kasischke ES, et al. (1992) Dependence of radar backscatter on coniferous forest biomass *IEEE Transaction on Geoscience and Remote Sensing* 30: 412–415.
51. Le Toan T, Beaudoin A, Riom J, Guyon D (1992) Relating Forest Biomass to SAR Data *IEEE Trans Geosci Remote Sensing* 30: 403–411.
52. Rignot E, Way J (1994) Monitoring freeze-thaw cycles along north-south Alaskan transects using ERS-1 SAR *Remote Sensing of Environment*, 49: 131–137.
53. Enghart S, Keuck V, Siegert F (2011) Aboveground biomass retrieval in tropical forests – the potential of combined X- and L-band SAT data use *Remote Sensing of Environment*, doi:10.1016/j.rse.2011.01.008.
54. Mitchard ETA, Saatchi SS, Lewis SL, Feldpausch TR, Woodhouse IH, et al. (2011) Measuring biomass changes due to woody encroachment and deforestation/degradation in a forest-savanna boundary region of central Africa using multi-temporal L-band radar backscatter *Remote Sensing of Environment*, doi:10.1016/j.rse.2011.02.022.
55. Avtar R, Herath S, Saito O, Gera W, Singh G, et al. (2013) Application of remote sensing techniques towards the role of traditional water bodies with respect to vegetation conditions. *Environment, Development and Sustainability*, DOI: 10.1007/s10668-013-9507-4.
56. Sun G, Ranson KJ, Guo Z, Zhang Z, Montesano P, et al. (2011) Forest biomass mapping from lidar and radar synergies *Remote Sensing of Environment*, doi:10.1016/j.rse.2011.03.021.
57. Cartus O, Santoro M, Kelldorfer J (2012) Mapping forest aboveground biomass in the northern United States with ALOS PALSAR dual-polarization L-band *Remote Sensing of Environment*, 124: 466–478.
58. UNEP (2009) Cambodia environment outlook Report published by Ministry of Environment, Kingdom of Cambodia.
59. Rajaona AM (2008) Comparative study of Allometric Parameters of Cashew tree (*anacardium occidentale*) In North East Brazil, Master thesis, University of Bonn.
60. Ashwall D, Ogonowski M, Neou S, McCulloch C (2011) Assisting Cambodian policymakers with designing REDD plus approaches under a post-2012 international climate change policy framework *Center for Clean Air Policy*: 45–47.
61. Cambodia Agribusiness Series No 1 (2010) Prospects for Cambodia's cashew sub-sector *International Finance Corporation European Union*.
62. Gillis MD (2001) Canada's national forest inventory (Responding to current information needs) *Environmental Monitoring Assessment*, 67: 121–129.

63. Rosenqvist A, Shimada M, Ito N, Watanabe M (2007) ALOS PALSAR: A Pathfinder mission for global-scale monitoring of the environment *IEEE Transactions on Geoscience and Remote Sensing*, 45(11): 3307–3316
64. Islam Md N, Kurttila M, Mehtatalo L, Pukkala T (2010) Inoptimality losses in forest management decisions caused by errors in an inventory based on airborne laser scanning and aerial photographs *Canadian Journal of Forest Research*, 40: 2427–2438.
65. Kongrattachok P (2005) Carbon sequestration in cassava and para rubber plantation, Rayong province Master thesis, Mahidol University.
66. Kiyono Y, Furuya N, Sum T, Umemiya C, Itoh E, et al. (2010) Carbon stock estimation by forest measurement contributing to sustainable forest management in Cambodia *JARQ*, 44, 1: 81–92
67. Shimada M, Isoguchi O, Tadono T, Isono K (2009) PALSAR polarimetric calibration and geometric calibration *IEEE, Transactions on Geoscience and Remote Sensing*, 47, 12: 3915–3932.
68. Avtar R, Takeuchi W, Sawada H (2013) Full Polarimetric PALSAR based Land Cover Monitoring in Cambodia for Implementation of REDD Policies *International Journal of Digital Earth*, 6, 3: 255–275.
69. Mitchard ETA, Saatchi SS, Woodhouse IH, Nangendo G, et al., (2009) Using satellite radar backscatter to predict above-ground woody biomass: a consistent relationship across four different African landscapes *Geophysical Research Letters*, 36, L23401 doi:10.1029/2009GL040692
70. Hamdan O, Aziz HK, Rahman KA (2011) Remotely sensed L-band SAR data for tropical forest biomass estimation *Journal of Tropical Forest Science*, 23, 3: 318–327.
71. Hair JR, Anderson RE, Tatham RL, Black WC (1998) *Multivariate data analysis*, 5th Ed Prentice Hall, Upper Saddle River, NJ 730.
72. Avtar R, Takeuchi W, Sawada H (2011) Plantation based biomass estimation for REDD policies implementation in Cambodia, Synthetic Aperture Radar (AP SAR), 2011 3rd International Asia-Pacific Conference on, vol., no. pp.1,4, 26–30 Sept. 2011.
73. Avtar R, Takeuchi W, Sawada H (2011) Assessment of Cashew and Rubber plants biophysical parameters based on ALOS/PALSAR data *Seisan-Kenkyu*, 63, 4, 51–54.
74. Le Toan T, Quegan S, Davidson MWJ, Balzter H, Paillou P, et al. (2011) The BIOMASS mission: Mapping global forest biomass to better understand the terrestrial carbon cycle *Remote Sensing of Environment*, 115: 2850–2860.